Surface Analysis of Porcelain Fused to 4 Base Metal Alloys Using X-Ray Photoelectron Spectroscopy

X-Işını Fotoelektron Spektroskopisiyle 4 Farklı Temel Porselen Metali Alaşımının Yüzey Analizi

Tuncer Burak ÖZÇELİK,[a]
Bora BAĞIŞ,[b]
Işıl ÖZCAN,[a]
Pervin İMİRZALIOĞLU[a]

[a]Department of Prosthodontics, Başkent University, Faculty of Dentistry, Ankara,
[b]Department of Prosthodontics, Karadeniz Technical University, Faculty of Dentistry, Trabzon

Geliş Tarihi/*Received:* 04.11.2009
Kabul Tarihi/*Accepted:* 23.02.2010

Yazışma Adresi/*Correspondence:*
Tuncer Burak ÖZÇELİK
Başkent University, Faculty of Dentistry, Department of Prosthodontics, Ankara, TÜRKİYE/TURKEY
tbozcelik@yahoo.com

ABSTRACT Objective: The aim of this study is to determine the compositional surface changes of 4 different base metal alloys during surface preparation stages of the metal ceramic restorations. **Material and Methods.** Four commercial base metal alloys used in metal ceramic restoration were investigated in the study. A total of 12 round plastic patterns were used to fabricate the metal specimens, 16 mm in diameter and 1 mm thick. The cast metals surface was examined with the X-ray photoelectron spectroscopy (XPS) during the 3 stages of fabrication process of the metal ceramic restorations. These stages were smooth grinding and abrasion with airborne particles of 110-µm aluminum oxide, oxidation firing, and firing cycle for opaque ceramic applications. Besides, Energy dispersive X-ray analysis (EDAX) was performed to determine the constituent elements of the cast metal alloys after the abrasion stage. **Results:** Survey spectra by XPS of alloys showed some differences in the atomic percentages of elements among the evaluated stages. In the 3 stages, supporting the EDAX findings, aluminum was seen at the surface of the alloys. At the oxidation stage and opaque ceramic firing stage chromium and oxygen concentrations were increased for all of the investigated alloys` surfaces. **Conclusion:** Surface composition of examined alloys is very different from the manufacturers' reported batch compositions. Oxides were present in more than 1 form on the surface at the oxidation and opaque porcelain firing stages, depending on the binding energy level. Aluminum oxide was detected on the surface of all alloys during the 3 preparation stages.

Key Words: Metal ceramic alloys; Spectrometry, X-ray emission; X-ray diffraction

ÖZET Amaç: Bu çalışmanın amacı, 4 farklı temel metal alaşımının, metal seramik restorasyonlarının hazırlıkları sırasında, yüzeylerinde meydana gelen kompozisyonel değişimlerin belirlenmesidir. **Gereç ve Yöntemler:** Metal seramik restorasyonlarında kullanılan ve ticari olarak mevcut olan 4 farklı temel metal alaşımı incelenmek üzere çalışmamızda kullanılmıştır. 16 mm genişliğinde ve 1 mm kalınlığındaki metal örneklerini oluşturmak için 12 tane yuvarlak plastik yapılmıştır. Dökümleri yapılmış metal örneklerinin yüzeyleri, metal seramik restorasyonların yapım sürecinde 3 aşamada X-ışını fotoelektron spektroskopisi ile incelenmiştir. Bu aşamalar metal tesfiyesi ve 110-µm aluminyumoksit partikülü ile kumlama, oksidasyon fırınlaması ve opak seramik fırınlamasıdır. Aynı zamanda enerji ayrımlı X-ışını ile tesfiye sonrası metal örneklerin yüzey bileşenleri de incelenmiştir. **Bulgular:** X-ışını fotoelektron spektroskopisi (XPS) ile değerlendirilen aşamalar arasında elementlerin atomik yüzdelerinde farklılıklar belirlenmiştir.Her 3 aşamada da enerji ayrımlı X-ışını (EDAX) bulgularını destekleyecek şekilde metal yüzeylerinde aluminyuma rastlanmıştır. Tüm incelenen metallerde oksidasyon ve opak fırınlaması aşamalarında krom ve oksijen konsantrasyo- nunun yüzeyde arttığı görülmüştür. **Sonuç:** İncelenen alaşımların yüzey kompozisyonları üretici firmaların bildirdiği içerikten farklılık göstermektedir. Oksidasyon ve opak fırınlaması aşamalarında metal yüzeyinde bulunan oksitler bağlanma enerjilerine bağlı olarak birden fazla formda bulunmaktadırlar. Ayrıca her 3 aşamada da metal alaşımlarının yüzeyinde aluminyum oksit belirlenmiştir.

Anahtar Kelimeler: Metal seramik alaşımlar; Spektrometri, X ışını yayınım; X-ışını kırılması

Turkiye Klinikleri J Dental Sci 2011;17(1):8-16

The primary requirement for the success of metal ceramic restoration is development of a durable bond between the ceramic and the alloy.[1] Thus, formation of an oxide layer at the alloy surface is vital to metal ceramic bonding.[1-4] Many studies have been published about how to form the oxide layer to optimize bonding.[4-14] Research suggests that an oxide layer of less than 1 to 2 nm provides good bonding and sandblasting with aluminum oxide (Al_2O_3) particles is one of the surface treatments that improves bonding.[8-14]

The oxidation behavior of dental alloys largely determines their potential for bonding with porcelain. Research into the nature of metal porcelain adherence indicates that adherence of the oxide during the oxidation firing stage determines the quality of resultant ceramic metal bond,[15,16] and this stage appears to be an essential part of the alloy preparation because it brings to the surface elements that would otherwise not be there.[10,17]

Differences in the amounts of minor elements could significantly affect the oxidation rate of the alloy and the reaction with the ceramic.[11,18-20] In general, metal oxides are easily produced for base metal alloys under high temperature, and the thickness of the oxide layer is dependent on the degree of oxidation of metal elements in the alloy.[21] If the oxide layer is too thick, the metal surface is prone to fracture during the ceramic firing process. Therefore, the effect of the chemical composition of base metal alloys on the thickness of oxide layers is an important consideration.[22]

Nickel oxide and chromium oxide are the most abundant types of oxide products.[18,22] Aluminum is added to alloys to improve the degree of oxidation via formation of Al_2O_3, thus decreasing the thickness of the oxide layer.[13,18,22] For nickel-chromium alloys, the elements appearing at the surface after oxidation are chromium, manganese, and calcium.[17] Tin oxide provides continuity of the electronic structure between alloy and ceramic structures and is a primary factor in controlling metal ceramic adherence. Chemical bonding is maximized when a monomolecular oxide layer is maintained.[3]

Most reports have studied the metal ceramic interface. However, none of those studies has focused on metal alloy surface. In the 1 report that did study the metal alloy surface, Johnson et al. found surface alterations after 4 different metal ceramic alloy surface preparations that are commonly performed for nickel-chromium and palladium-silver alloys. The surface composition of metal ceramic alloys was dramatically different from their bulk composition through the preparation stages.[17]

Although base metal alloys have similar compositions and mechanical properties, important differences are observed when they are cast and bonded to ceramic.[18] Therefore; knowledge of the composition and elemental changes is of great importance for optimizing the ceramic fused to metal during processing. The present study was done to determine the compositional surface changes of 4 different base metal alloys at preparation stages before and during ceramic application, using energy dispersive X-ray analysis (EDAX) and X-ray photoelectron spectroscopy (XPS).

The null hypothesis of this study was that the surface composition of metal ceramic alloys would be similar with their bulk composition through the preparation stages.

MATERIAL AND METHODS

Four commercial base metal dental casting alloys used in metal ceramic restoration were investigated: 2 nickel-chromium alloys (Argeloy N.P., Heranium NA) and 2 cobalt-chromium (Metalloy CC, Microlit isi) alloys. The bulk compositions for the alloys are listed in Table 1. From each alloy, 3 round specimens were prepared. A total of 12 round plastic patterns (Essix A+ .040; Raintree Essix, Inc, Metairie, LA) were used to fabricate the metal specimens, 16 mm in diameter and 1 mm thick. Specimens were sprued, invested with a phosphate- bonded investment (AlphaCast Vario; Schütz Dental Group, Rosbach, Germany), and cast according to each manufacturer's instructions. The alloys were melted with a gas-oxygen torch and cast in a centrifugal casting machine. Each specimen was abraded with airborne particles of 250-μm Al_2O_3 (Korox 250; BEGO, Bremen, Germany)

TABLE 1: Composition of metal ceramic alloys selected for investigation.

Alloy Groups	Product names (Lot Numbers)	Codes	Composition (%)	Manufacturer
Nickel-Chromium	Argeloy N.P. (2486525)	ANP	76 Ni, 14 Cr, 6 Mo, 1.8 Be, 2 Al, others	Argen Corporation, San Diego, CA, USA
	Heranium NA (12446)	HNA	59.3 Ni, 24 Cr, 10 Mo, Fe<2, Mn<2, Ta<2, Si<2, Nb<2	Heraeus Kulzer, Hanau, Germany
Cobalt-Chromium	Metalloy CC (156)	MCC	61.5 Co, 27.5 Cr, 1.3 Si, 8.6 W, Mn, N, Nb >1	Metalor, Neuchaptel, Switzerland.
	Microlit isi (2004004194)	Misi	61.1 Co, 27.8 Cr, 1.7 Si, 0.3 Mn, 8.5 W	Schütz Dental Group, Rosbach, Germany

Note: Alloy compositions provided by indicated manufacturers.

to remove the investment material. The sprues were cut off, and the specimens were adjusted with tungsten carbide rotary cutting instruments (H138FSQ; Komet, Lemgo, Germany), abraded with airborne particles of 110-μm Al_2O_3 (Basic Classic; Renfert GmbH, Hilzingen, Germany), and steam cleaned (VAP 6-A; Emmevi SpA, Badia Polesine, Italy). The specimens were oxidized (Programat X1; Ivoclar Vivadent, Schaan, Liechtenstein) according to the manufacturers' recommendations (Table 2).

The alloys were subjected to an opaque ceramic firing cycle and dried at a temperature of 403°C for 6 minutes. The rate of the temperature rise was 80°C/min. The vacuum started at 450°C and finished at 899°C. Peak temperature was 900°C, at which the specimens were held for 1 minute. The second opaque porcelain firing cycle differed in the final temperature of the vacuum (889°C) and in the peak temperature (890°C).

The cast metal surface was examined with XPS during the 3 stages of the fabrication process of the metal ceramic restorations. These stages are smooth grinding and abrasion with airborne particles of 110-μm Al_2O_3 (Korox, BEGO) (referred to as the abrasion stage), oxidation firing (the oxidation stage), and firing cycle for opaque ceramic applications (the opaque ceramic firing stage). The abrasion and oxidation stages are identical with the fabrication steps used for metal ceramic restorations. The opaque ceramic firing stage was added to match the same temperature program used for fusing opaque ceramic but without the application of opaque ceramic. EDAX analysis was only performed to determine the constituent elements of the cast metal alloys after the abrasion stage.

To analyze the changes in surface compositions of the specimens, XPS was performed (SPECS ESCA; Berlin, Germany) with magnesium-aluminum dual anode using magnesium Kα radiation operated at 10 kV and 250 W. The hemispheric electrostatic energy analyzer, which was equipped with a multichannel detector with 18 discrete channels, operated in the constant pass energy mode. A survey spectrum was evaluated at pass energy of 96 eV and detailed spectra were obtained at 48 eV pass energy. The spectrometer was operated in constant analyzer energy mode. Pressure of the analyzer chamber was 10 to 8, to 10 to 9 torr. The binding energies for all spectra were referenced by assuming that the major component of the carbon peak resulted from hydrocarbon contamination at a binding energy of 285 eV.

TABLE 2: Oxidation cycle specifications recommended by manufacturers.

Brand Names	Code	Temperature	Vacuum	Minutes Held	
Argeloy NP	ANP	650-980ºC	Yes	0	Abraded with airborne particles of 110-μm aluminum oxide before opaque porcelain application.
Heranium NA	HNA	950-980ºC	Yes	5	
Metalloy CC	MCC	Not recommended			
Microlit isi	Misi	980ºC	Yes	5	

RESULTS

Figures 1A, B, C, and D show the EDAX of cast alloys after the abrasion stage. There were some differences between the alloy manufacturers' reported compositions and the EDAX of semi quantitative compositions of the cast and sandblasted alloys (Table 3). The most remarkable difference was the presence of aluminum (between weight 9.24% to 14.11% and atom 12.44% to 16.20%) in the abrasion stage, in comparison to the manufacturer's data.

Survey spectra by XPS were used to determine the relative concentrations of elemental components present on the alloy surfaces and to identify their chemical composition in the alloy preparation stages. Tables 4, 5, 6, and 7 summarize the elemental percentages (atom %), orbits, binding energy ranges, and possible chemical status of the surface of base metal alloys based on XPS analyses of the test specimens for alloy preparation stages. Surface analysis of base dental alloys by XPS showed some differences in the atomic percentages of elements in the 3 stages.

The most intense photoelectron peak for each element was used for quantification; carbon (C 1s), oxygen (O 1s), aluminum (Al 2p), nickel (Ni 2p), chromium (Cr 2p), cobalt (Co 2p), silicon (Si 2p), molybdenum (Mo 3d), manganese (Mn 2p), and tungsten (W 4f). Distributions of binding energy on the surfaces of the nickel-chromium and cobalt-chromium alloys at the preparation stages obtained by XPS analysis are presented in Figures 2 and 3.

In the 3 stages, supporting the EDAX findings, aluminum was seen at the surface of the alloys (between 4.5% and 31.9%), compared to data provided by the manufacturers in Table 1. Aluminum atomic percentages decreased in the oxidation and porcelain firing stages for all alloys. An aluminum peak was present on all alloy surfaces with binding en-

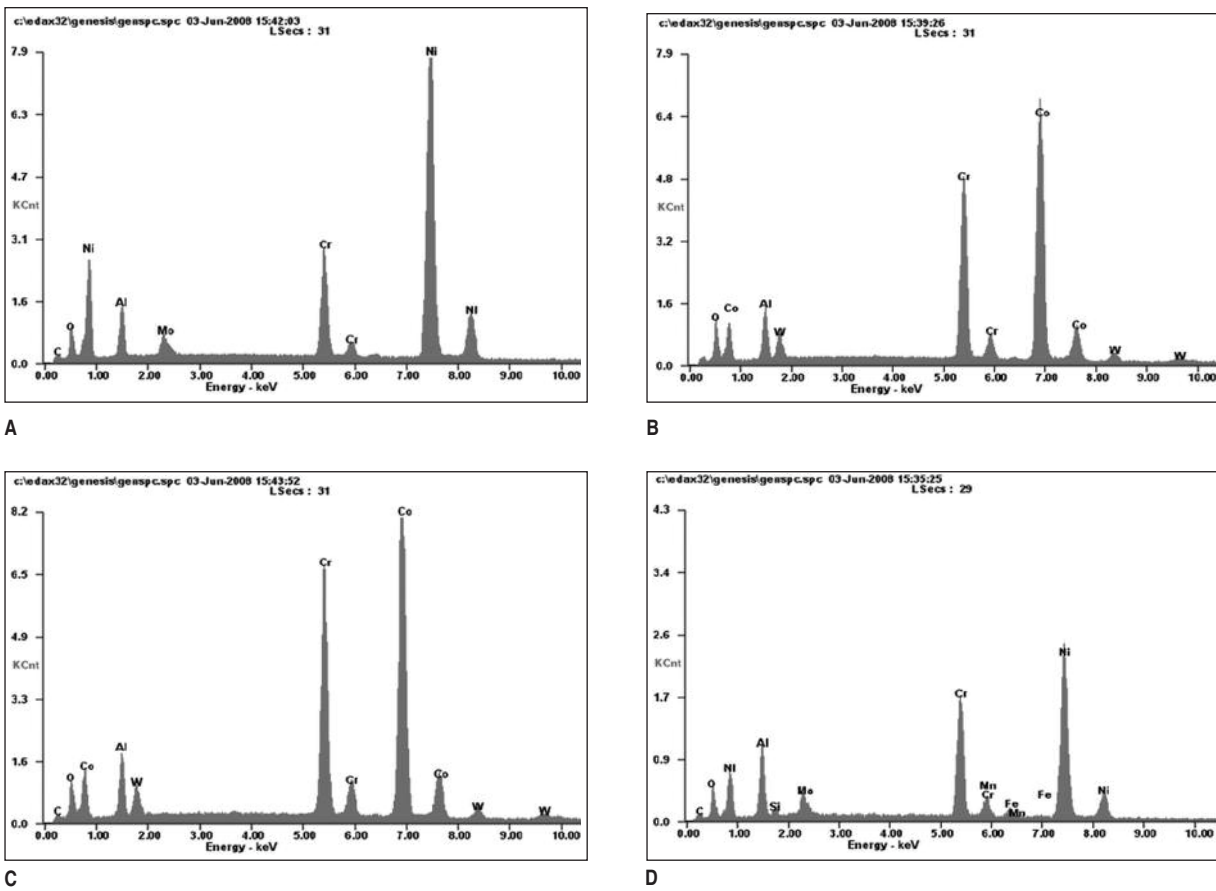

FIGURE 1: A, B, C ve D. EDAX analysis of cast base metal alloys after smooth grinding and abrasion with airborne particles of 110-µm aluminum oxide.

TABLE 3: Elemental composition of metal ceramic alloys obtained from EDAX.

	ANP		HNA		MCC		Misi	
Elements	**Weight (Wt %)**	**Atom (At %)**	**Weight (Wt %)**	**Atom (At %)**	**Weight (Wt %)**	**Atom (At %)**	**Weight (Wt %)**	**Atom (At %)**
Al	9.62	12.44	14.11	16.20	9.24	12.68	10.28	15.62
Ni	56.35	33.47	38.16	20.14	_	_	_	_
Cr	10.76	7.22	15.33	9.14	21.92	15.62	21.10	16.63
Co	_	_	_	_	47.15	29.63	49.73	34.58
Mo	5.15	1.87	6.50	2.10	_	_	_	_
Si	_	_	1.38	1.53	_	_	_	_
Mn	_	_	0.79	0.44	_	_	_	_
W	_	_	_	_	6.04	1.22	6.50	1.45
Fe	_	_	1.08	0.60	_	_	_	_

– Could not be detected by EDAX.

TABLE 4: XPS Elemental analysis of test specimens for 3 preparation stages of the ANP nickel-chromium alloy.

	Abrasion Stage			Oxidation Stage			Porcelain Firing Stage			Possible Chemical Status
Elements	**Atom (%)**	**Orbit**	**BER (eV)**	**Atom (%)**	**Orbit**	**BER (eV)**	**Atom (%)**	**Orbit**	**BER (eV)**	
C	31.9	1s	292-280.7	14.0	1s	292-280.7	19	1s	292-279.8	_
O	36.7	1s	537.2-527.2	53.2	1s	536.6-525.5	51.2	1s	537.2-525.5	_
Al	8.6	2s	125.5-115.7	6.5	2s	125.4-115.4	7.3	2s	128-115.7	Al2O3 (75.8 eV)
Ni	12.1	2p	878.1-847.7	18.9	2p	878.1-847.7	14.3	2p	878.1-847.7	Ni (852.5 eV), NiO (853.5 eV), Ni2O3 (855.7 eV)
Cr	4.8	2p	586.2-570.7	4.8	2p	593-570.7	5.2	2p	594.1-569	Cr (573.6 eV), Cr2O3 (575.6 eV), CrO2 (575.9 eV), CrO3 (577.9 eV)
Si	4.8	2p	107.2-97.5	2.3	2p	106.7-97.2	2.7	2p	106.3-95.5	Si (98.6 eV), SiO2 (102.5 eV)
Mo	1.1	3d	234.8-225.7	0.4	3d	238.8-224.4	0.3	3d	240.2-225	Mo (231.2 eV), MoO3 (235.5 eV)

BER, Binding Energy Range (eV).

TABLE 5: XPS elemental analysis of test specimens for 3 preparation stages of the HNA nickel-chromium alloy.

	Abrasion Stage			Oxidation Stage			Porcelain Firing Stage			Possible Chemical Status
Elements	**Atom (%)**	**Orbit**	**BER(eV)**	**Atom (%)**	**Orbit**	**BER (eV)**	**Atom (%)**	**Orbit**	**BER (eV)**	
C	11.4	1s	294.5-280.7	8.8	1s	292-280.7	4.5	1s	292-279.8	_
O	24.0	1s	535.3-527.7	57.9	1s	536.6-525.5	63.1	1s	537.2-525.5	_
Al	18.0	2s	128-115.7	10.1	2s	125.4-115.4	9.3	2s	128-115.7	Al2O3 (75.8 eV)
Ni	34.3	2p	874.7-849.1	1.7	2p	874.2-848.5	1.2	2p	878.1-847.7	Ni (852.5 eV), NiO (853.5 eV), Ni2O3 (855.7 eV)
Cr	10.7	2p	589.6-569.6	10.6	2p	593-569	12.1	2p	594.1-569	Cr (573.6 eV), Cr2O3 (575.6 eV), CrO2 (575.9 eV), CrO3 (577.9 eV)
Mo	1.6	3d	237.6-226	0.2	3d	237.7-227.2	_	_	_	Mo (231.2 eV), MoO3 (235.5 eV)
Mn	_	_	_	10.7	2p	657.2-635.3	9.7	2p	658.7-635.3	Mn (638.8 eV), Mn0 (641 eV), Mn2O3 (641.1 eV), Mn3O4 (641.2 eV), MnO2 (642 eV)

BER, Binding Energy Range (eV).

TABLE 6: XPS elemental analysis of test specimens for 2 preparation stages of the MCC cobalt-chromium alloy.

	Abrasion Stage			Porcelain Firing Stage			Possible Chemical Status
Elements	Atom (%)	Orbit	BER (eV)	Atom (%)	Orbit	BER (eV)	
C	24.9	1s	292-280.7	24.0	1s	292-280.7	_
O	22.9	1s	535.2-527.2	45.0	1s	538.1-527.2	_
Al	8.8	2s	128-115.7	4.2	2s	128-115.7	Al2O3 (75.8 eV)
Co	22.0	2p	798.5-773.6	9.6	2p	799.3-773.6	Co (778.2 eV), Co2O3 (779.2 eV), Co3O4 (780.3 eV)
Cr	3.8	2p	591.2-568.7	8.7	2p	591.5-569.2	Cr (573.6 eV), Cr2O3 (575.6 eV), CrO2 (575.9 eV), CrO3 (577.9 eV)
Mn	5.2	2p	660.7-628.1	0.8	2p	660.7-633.2	Mn (638.8 eV), Mn0 (641 eV), Mn2O3 (641.1 eV), Mn3O4 (641.2 eV), MnO2 (642 eV)
Si	11.0	2p	108.7-95.5	7.2	2p	108.7-95.5	Si (98.6 eV), SiO2 (102.5 eV)
W	0.8	4f	38.7-28.8	0.3	4f	40.2-30.2	W (30.8 eV), WO2 (32.4 eV), WO3 (35.2 eV)

BER, Binding Energy Range (eV).

TABLE 7: XPS elemental analysis of test specimens for 3 preparation stages of the Misi cobalt-chromium alloy.

	Abrasion Stage			Oxidation Stage			Porcelain Firing Stage			Possible Chemical Status
Elements	Atom (%)	Orbit	BER (eV)	Atom (%)	Orbit	BER (eV)	Atom (%)	Orbit	BER (eV)	
C	29.9	1s	292.5-279	15.6	1s	291.2-280	23.5	1s	292-280.7	_
O	25.6	1s	534-526.1	38.5	1s	535.2-524.8	42.5	1s	535.2-527.2	_
Al	9.9	2s	125.2-114.9	7.8	2p	79.2-69.7	2.5	2s	128-115.7	Al2O3 (75.8 eV)
Co	17.3	2p	796.7-774.1	18.5	2p	799.1-771.1	13.4	2p	799.7-773.6	Co (778.2 eV), Co2O3 (779.2 eV), Co3O4 (780.3 eV)
Cr	3.4	2p	590.3-568.7	10.1	2p	591.5-570.5	9.7	2p	592.6-570.1	Cr (573.6 eV), Cr2O3 (575.6 eV), CrO2 (575.9 eV), CrO3 (577.9 eV)
Mn	3.4	2p	651.1-631.1	2.7	2p	657.7-631.7	2.2	2p	657.7-631.7	Mn (638.8 eV), Mn0 (641 eV), Mn2O3 (641.1 eV), Mn3O4 (641.2 eV), MnO2 (642 eV)
Si	10.2	2p	108-96	5.0	2p	108.7-95.5	5.5	_	108.7-95.5	Si (98.6 eV), SiO2 (102.5 eV)
W	0.3	4f	38.7-28.8	0.7	4f	38.7-28.8	4f	0.7	38.7-28.8	W (30.8 eV), WO2 (32.4 eV), WO3 (35.2 eV)

BER, Binding Energy Range (eV).

ergies that correlated with aluminum oxide (75.8 eV). After the oxidation and opaque ceramic firing stages, XPS scans demonstrated the presence of Al_2O_3 on the surfaces of the alloys. However, the peak for aluminum was slightly reduced.

High levels of carbon and oxygen were detected in the 3 stages, which is typical for all XPS analyses. The presence of carbon is due to organic species adsorbed on the high-energy oxide surface. For all alloy groups, the carbon ratio decreased from the first stage (abrasion) to the last stage (opaque ceramic firing). The oxygen (O 1s) peaked in the oxidation and opaque ceramic firing stages,

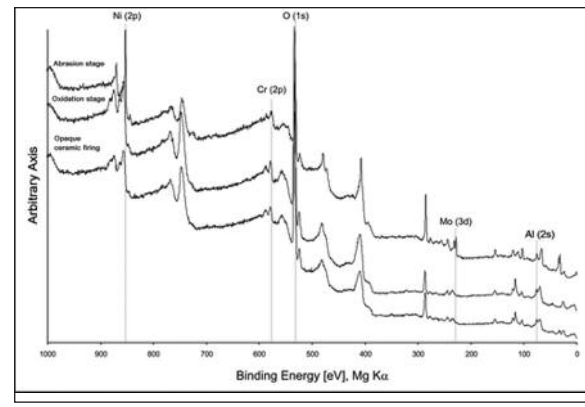

FIGURE 2: Survey spectra by XPS from the ANP nickel-chromium alloy. Peaks for the alloy's major components are shown for the abrasion stage, oxidation stage, and porcelain firing stage.

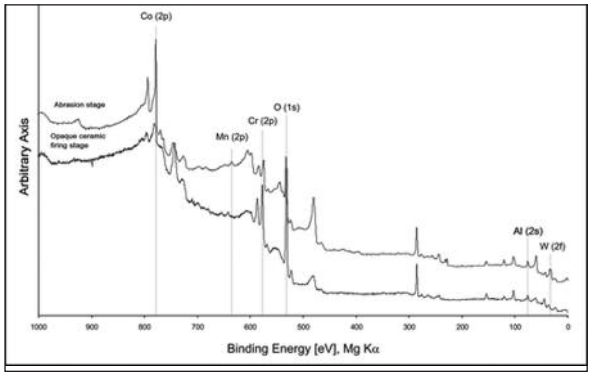

FIGURE 3: Survey spectra by XPS from the MCC cobalt-chromium alloy. Peaks for the alloy's major components are shown for the abrasion stage and porcelain firing stage.

in association with the oxygen ratio increasing in those 2 stages. A possible reason might be the oxide compounds occurring with heat application on the alloy surfaces. For all alloys, the oxygen peak exhibited a broad asymmetric shape, indicating the presence of both metal oxides and hydroxides on the alloy surfaces. The reason for the absence of MCC alloy in the oxidation stage is related to the manufacturer's recommendation. This product does not need a separate oxidation stage.

When evaluating the 2 nickel-chromium alloys (Argeloy N.P. and Heranium NA), major elements detected on the surfaces were chromium, nickel, silicon, manganese, and molybdenum at the abrasion stage. Surface evaluation indicated that while the percentage of chromium increased in the oxidation and porcelain firing stages for both nickel-chromium alloys, the percentage of nickel increased for ANP but decreased for HNA. Molybdenum percentages decreased in the oxidation and porcelain firing stages (Tables 4, 5). The peak for beryllium was not detected, although the ANP alloy includes beryllium in its composition.

Major elements detected on the surfaces of the 2 cobalt-chromium alloys (Metalloy CC and Microlit isi) were cobalt, chromium, manganese, tin, and tungsten in the abrasion stage. Chromium percentages in the oxidation and porcelain firing stages increased. Tungsten percentages decreased in the MCC alloy but increased in the Misi alloy. Percentages of all other elements decreased in the oxidation and porcelain firing stages (Tables 6, 7). For the B3 alloy, for which oxidation is not recommended, the chemical status and percentage of elements on the surface after opaque ceramic firing were similar to the Misi alloy that requires oxidation.

Tables 4, 5, 6, and 7 show the compositional data and possible chemical status of the alloys' surfaces based on XPS analyses of 3 test specimens for the 4 different alloys used at the 3 stages of metal porcelain construction. The binding energy analysis of the alloys with XPS showed the estimated forms of the elements and atoms.

DISCUSSION

Only 1 study has addressed changes on the metal surface during ceramic preparation stages.[17] Therefore, changes in the surface properties of base metal alloys during metal surface preparation of metal ceramic restorations were analyzed in this study. The null hypothesis of this study was rejected as discrepancies on the surface composition of investigated metal ceramic alloys in comparison with their bulk compositions were noted and there were elemental changes on the surface of the alloys in different preparation stages. Statistical analysis was not carried out since XPS analysis does not provide numerical values and examinations of surface properties changes were aimed only in this study.

The results of this study show that metal preparation stages are important for nickel-chromium and cobalt-chromium alloys to release a sufficient proportion of some elements (eg, chromium) that contribute to the metal ceramic bond. These results are similar to the results of studies that show that alloy surface preparation affects surface elements present in the oxide layer.[6,7,10,12,13,17] Johnson et al evaluated palladium-silver and nickel-chromium alloys with XPS analyses. Chromium in the nickel-chromium alloy was not detected on the metal surface in the abrasion stage, whereas chromium increased in the oxidation and opaque ceramic firing stages.[17]

In current study, chromium was detected on the metal surface of all alloys, and it increased after the oxidation and opaque firing stages in both nickel-chromium and cobalt-chromium alloys. The authors believe that when heat is applied in the ox-

idation stage, chromium moves toward the surface to form a compound. Nickel in nickel-chromium alloys was observed on the surface in the 3 stages while cobalt was observed in cobalt-chromium alloys. However, compared with chromium, the amount of nickel and cobalt decreased after the oxidation and opaque firing stages. Chromium, nickel, and cobalt are the elements accounting for the largest proportion of the oxidation layer on the metal alloy surfaces. Elements in nickel-chromium and cobalt-chromium alloys that are commonly added to improve physical properties include molybdenum, tin, tungsten, beryllium, iron, tantalum, and manganese.[20]

Carbon is another element detected on the metal surface. The authors believe that the level of carbon seen on the surface of both nickel-chromium and cobalt-chromium alloys tested is due to organic species adsorbed on the high-energy oxide surface.

The amount of oxygen detected in XPS analysis increased gradually in the oxidation and opaque stages. The oxygen at the alloy surfaces was made up of elemental oxidation of most of the elements within the alloys. These oxides are present in different forms over metal alloys. Nickel was observed as oxides NiO and Ni_2O_3, cobalt as Co_2O_3 and Co_3O_4, and chromium as Cr_2O_3, CrO_2, and CrO_3. This conflicted with the observations of Anusavice and associates who found that only single metal oxides, such as Cr_2O_5 or NiO, were formed to induce ceramic metal adherence. However, findings similar to ours were reported by Johnson and associates, which support 1 of the conclusions of this study: that different forms of oxides exist over metal alloys.[2,17]

In previous studies, the oxide form seen most commonly in nickel-chromium alloys was $NiCr_2O_4$. Faster-growing NiO is usually found on the exterior of the oxide scale, Cr_2O_3 in the interior, covering the alloy, and $NiCr_2O_4$ between NiO and Cr_2O_3, formed as the product of a reaction between the 2 oxides.[2,18] The relative amounts of these oxides depend on the chromium concentration in the alloy.

Chromium oxide (Cr_2O_3) was found to be 1 of the main oxide forms that formed on the nickel-chromium alloys under high temperature in all 3 preparation stages. However, excessive Cr_2O_3 can cause changes in the thermal expansion coefficient of the porcelain layer that provoke internal stress; thus, bond strength between metal and ceramic may decrease.[18] In addition, pure chromium forms a poorly adherent oxide and is responsible for loss of oxide adherence in chromium-containing alloys. Several theories have been advanced to explain the marked improvement in oxide adherence achieved by the addition of oxygen-active elements, such as aluminum, to chromium-containing alloys.[15] The added aluminum improves the degree of oxidation via the formation of Al_2O_3, which could efficiently hinder the growth of Cr_2O_3 and consequently decrease the thickness of the oxide layer.[13,18,22]

$Al_2O_3$was detected through the abrasion stage and remained on the surface of the metal alloys even though the amount decreased in the oxidation and opaque ceramic firing stages. The amount of Al_2O_3found at the alloy surface for all alloys was more than expected, which may be due to particles embedded during sandblasting. The influence of Al_2O_3 on the metal porcelain bond is not clear; however, some authors claim that Al_2O_3 enhances the strength of the metal ceramic bond.[12,13] Al_2O_3 is a metal oxide that exists in most porcelain powders. The aluminum oxide particles might have fused on the surface during porcelain firing, which might lead to increased adherence.

Molybdenum is the third most important element after nickel and chromium in nickel-chromium alloys. Molybdenum is a refractory metal and is not readily oxidized, but the oxide product of molybdenum (eg, MoO3) becomes volatile at temperatures exceeding 700°C.[18] Both nickel-chromium alloys used in this research contained molybdenum (6% to 10% by weight) in the bulk alloy (Table 1). The molybdenum content on the surface oxide layers for these nickel-chromium alloys after heat treatment at 980°C (oxidation stage) for up to 5 minutes was almost insignificant (0.2% to 0.4%) (Tables 4 and 5). After opaque firing stage, molybdenum content on the surface

oxide layers was decreased (0% to 0.2%). In our opinion, the decreased molybdenum content on the surface oxide layer may be due to the volatility of molybdenum oxide (MoO_3) during oxidation and opaque ceramic firing.

There may be some limitations since results are only valid for base metal ceramic alloys that we have examined in the present study. Additionally, SEM can be used together with XPS and EDAX to verify the outcomes and more specimens have been used. Future research is needed to understand the behavior of different metal alloys such as high noble and noble alloys.

CONCLUSION

The following conclusions were made:

1. Chromium concentrations increased on the surfaces of the base metal alloys during oxidation and opaque porcelain firing stages.

2. Oxides were present in more than 1 form on the surface of the base metal alloys at the oxidation and opaque porcelain firing stages, depending on the binding energy level.

3. Aluminum oxide was detected on the surface of all alloys during the 3 preparation stages.

4. Molybdenum content on the surface oxide layers for both nickel-chromium alloys after the oxidation and porcelain firing stages was almost negligible.

5. Although base metal alloys have similar compositions and mechanical properties, important differences are observed when they are cast and bonded to ceramic. Knowledge of the composition and elemental changes is of great importance for optimizing the ceramic fused to metal during processing for both clinicians and technicians. The role of the surface treatments and the preparation stages to obtain oxides should be well defined to improve bonding.

REFERENCES

1. McLean JW, Hubbard JR, Kedge MI. The Science and Art of Dental Ceramics. The Nature of Dental Ceramics and their Clinical Use; Monograph II: The strengthening of dental porcelain. 1st ed. Chicago: Quintessence Publishing Co; 1979. p.69-92.
2. Anusavice KJ, Ringle RD, Fairhurst CW. Adherence controlling elements in ceramic-metal systems. II. Nonprecious alloys. J Dent Res 1977;56(9):1053-61.
3. Anusavice KJ, Ringle RD, Fairhurst CW. Bonding mechanism evidence in a ceramic-nonprecious alloy system. J Biomed Mater Res 1977;11(5):701-9.
4. Carter JM, Al-Mudafar J, Sorensen SE. Adherence of a nickel-chromium alloy and porcelain. J Prosthet Dent 1979;41(2):167-72.
5. Bagby M, Marshall SJ, Marshall GW Jr. Metal ceramic compatibility: a review of the literature. J Prosthet Dent 1990;63(1):21-5.
6. Jochen DG, Caputo AA, Matyas J. Effect of metal surface treatment on ceramic bond strength. J Prosthet Dent 1986;55(2): 186-8.
7. Dent RJ, Preston JD, Moffa JP, Caputo A. Effect of oxidation on ceramometal bond strength. J Prosthet Dent 1982;47(1): 59-62.
8. Smith TB, Kelly JR, Tesk JA. In vitro fracture behavior of ceramic and metal–ceramic restorations. J Prosthodont 1994;3(3): 138-44.
9. Ohno H, Araki Y, Endo K. ESCA study on dental alloy surfaces modified by Ga–Sn alloy. J Dent Res 1992;71(6):1332-9.
10. Brantley WA, Cai Z, Papazoglou E, Mitchell JC, Kerber SJ, Mann GP, et al. X-ray diffraction studies of oxidized high-palladium alloys. Dent Mater 1996;12(6):333-41.
11. Değer S, Caniklioglu MB. Effects of tin plating on base metal alloy-ceramic bond strength. Int J Prosthodont 1998;11(2):165-72.
12. Wagner WC, Asgar K, Bigelow WC, Flinn RA. Effect of interfacial variables on metal-porcelain bonding. J Biomed Mater Res 1993;27(4):531-7.
13. Wu Y, Moser JB, Jameson LM, Malone WF. The effect of oxidation heat treatment of porcelain bond strength in selected base metal alloys. J Prosthet Dent 1991;66(4): 439-44.
14. Carter JM, Al-Mudafar J, Sorensen SE. Adherence of a nickel–chromium alloy and porcelain. J Prosthet Dent 1979;41(2):167–72.
15. Mackert JR Jr, Parry EE, Hashinger DT, Fairhurst CW. Measurement of oxide adherence to PFM alloys. J Dent Res 1984;63(11):1335-40.
16. Mackert JR Jr, Ringle RD, Parry EE, Evans AL, Fairhurst CW. The relationship between oxide adherence and porcelain-metal bonding. J Dent Res 1988;67(2):474-8.
17. Johnson T, van Noort R, Stokes CW. Surface analysis of porcelain fused to metal systems. Dent Mater 2006;22(4):330-7.
18. Baran GR. Oxide compounds on Ni-Cr alloys. J Dent Res 1984;63(11):1332–4.
19. Pask JA, Tomsia AP. Oxidation and ceramic coatings on 80Ni20Cr alloys. J Dent Res 1988;67(9):1164–71.
20. Kelly JR, Rose TC. Nonprecious alloys for use in fixed prosthodontics: a literature review. J Prosthet Dent 1983;49(3):363-70.
21. Berlotti RL. Porcelain-to-metal bonding and compatibility. In: McLean JW, ed. Dental Ceramics: Proceedings of the First International Symposium on Ceramics. Chicago: Quintessence Publishing Co; 1983. p. 415-41.
22. Huang HH, Lin MC, Lee TH, Yang HW, Chen FL, Wu SC, et al. Effect of chemical composition of Ni-Cr dental casting alloys on the bonding characterization between porcelain and metal. J Oral Rehabil 2005;32(3):206-12.